Photoinduced Charge Transfer in Porphyrin–Cobaloxime and Corrole–Cobaloxime Hybrids

ARTICLE *in* THE JOURNAL OF PHYSICAL CHEMISTRY C · DECEMBER 2012

Impact Factor: 4.77 · DOI: 10.1021/jp311766s

THE JOURNAL OF PHYSICAL CHEMISTRY C

Article

pubs.acs.org/JPCC

Photoinduced Charge Transfer in Porphyrin–Cobaloxime and Corrole–Cobaloxime Hybrids

Katrin Peuntinger,[†,¶] Theodore Lazarides,[‡,§,¶] Dimitra Dafnomili,[‡] Georgios Charalambidis,[‡] Georgios Landrou,[‡] Axel Kahnt,[†] Randy Pat Sabatini,[∥] David W. McCamant,[∥] Daniel T. Gryko,*[,⊥] Athanassios G. Coutsolelos,*[,‡] and Dirk M. Guldi*[,†]

[†]Department of Chemistry and Pharmacy, Interdisciplinary Center for Molecular Materials (ICMM), Friedrich-Alexander-Universitaet Erlangen-Nuernberg, Egerlandstrasse 3, 91058 Erlangen, Germany

[‡]Chemistry Department, University of Crete, Voutes Campus, PO Box 2208, 71003 Heraklion, Crete, Greece

[∥]Department of Chemistry, University of Rochester, Rochester, New York 14627, United States

[⊥]Institute of Organic Chemistry, Polish Academy of Sciences, Kasprzaka 44/52, 01-224 Warsaw, Poland

Supporting Information

ABSTRACT: We report on the synthesis of hybrid molecules consisting of a porphyrin or corrole chromophore axially coordinated to a $[Co^{III}(dmgH)_2(Cl)]^{\pm 0}$ (dmg = dimethylglyoxime) unit via a pyridine group as potential hydrogen forming entities in H_2O/THF medium. Photophysical, electrochemical, and pulse radiolysis studies on the hybrids and/or their separate components show that selective excitation of the porphyrin or corrole chromophore in its first singlet excited state leads to fast charge separation due to chromophore to cobalt electron transfer. However, this charge separation is followed by even faster charge recombination thereby preventing the accumulation of a reduced cobalt species which would lead to hydrogen production. It is important, nevertheless, that addition of a sacrificial electron donor slows the charge recombination down. In light of the latter it comes as hardly surprising that the photocatalysis experiments in the presence of a sacrificial electron donor (i.e., triethylamine) show modest rates of hydrogen production.

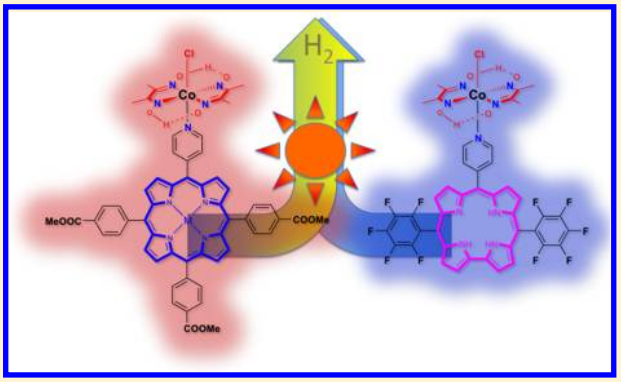

INTRODUCTION

With the global energy demand constantly rising, the need for developing new abundant and environmentally benign sources of energy is ever increasing.[1−3] Consequently, solar energy is expected to play an increasingly important role in the future. One of the major strategies for solar energy conversion is the production of hydrogen by the photocatalytic reduction of aqueous protons.[4,5] Hydrogen generation from photocatalytic systems is achieved through the reduction of a catalyst by photoinduced electron transfer from a sensitizer, which is regenerated by an electron donor.[1] Hydrogen production catalysts that have been studied in the literature include heterogeneous catalysts such as colloidal platinum[6−9] and molybdenum or tungsten sulfide[10−12] or homogeneous/molecular catalysts such as iron-based models of the enzyme hydrogenase.[13−16] Of particular interest for the electrochemically or photochemically driven generation of hydrogen are complexes belonging to the class of cobaloximes.[17−19] The catalytic mechanism is postulated to proceed through an active Co^{I} species formed by photochemical or electrochemical reduction of the initial $Co^{II/III}(dmgH)$ complex.[20,21] So far a number of such systems have been reported in the literature[1,17,22] with different photosensitizers including porphyrins,[23] other organic dyes,[24−27] $[Ru(bipy)_3]^{2+}$,[28] and platinum acetylide complexes.[7,29,30] The majority of the studies involve systems in which the sensitizer and catalyst are *not* chemically linked and their interaction is exclusively controlled by diffusion. However, there are several systems, which involve molecular conjugates, where sensitizer and catalyst are linked.[23,24,28] Whether or not such a conjugate improves the rates of hydrogen generation is still under debate. For example, Eisenberg and McCormick have recently reported that, in the case of a fluorescein sensitizer, connecting this chromophore to a cobaloxime actually leads to poorer performance in terms of hydrogen production. This is mainly attributed to the lability of the cobaloxime catalyst and to the reductive quenching mechanism, which is hampered when the chromophore is linked to the catalyst.[24] In this contribution, we report the synthesis of a series of electron donor–acceptor conjugates combining porphyrins or a corrole as photosensitizers with the

Received: November 29, 2012
Revised: December 12, 2012
Published: December 14, 2012

   dx.doi.org/10.1021/jp311766s | *J. Phys. Chem. C* 2013, 117, 1647−1655

Scheme 1. Schematic Overview of the Synthesis of 1Co, 2Co, and 3Co from 1, 2, and 3, Respectively

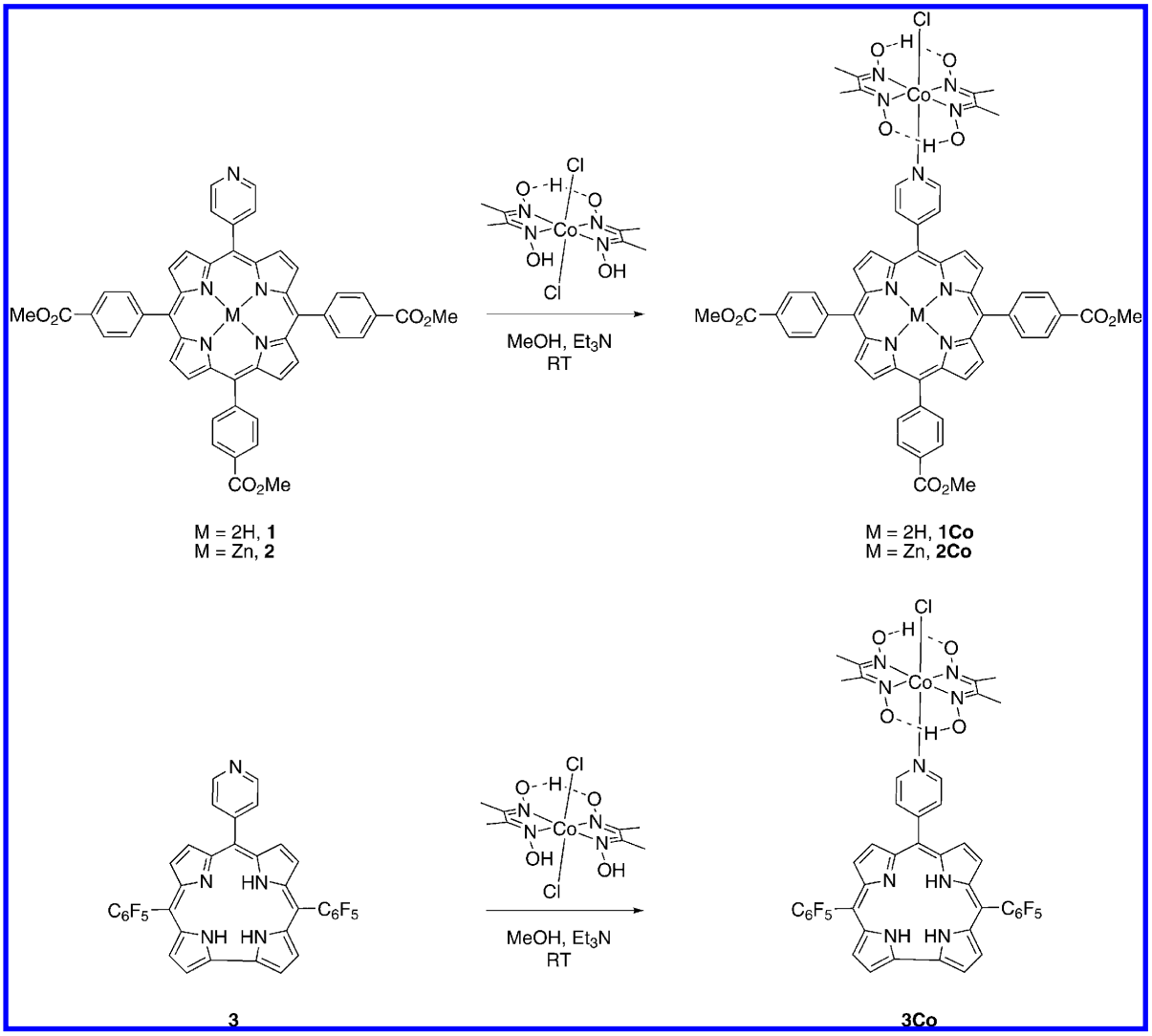

cobaloxime as catalyst. Spectroscopic investigations based on emission and transient absorption studies indicate that a fast and efficient photoinduced electron transfer from the singlet excited state of the porphyrins/corrole to the cobaloxime moiety takes place in the electron donor−acceptor conjugates. Notably, a fast charge recombination prevents further electron transfer to produce a catalytically active Co^{I} species. Despite the aforementioned, photocatalysis experiments in the presence of a sacrificial electron donor (i.e., triethylamine) show modest rates of hydrogen production.

EXPERIMENTAL SECTION

Materials. The chemicals were obtained from common commercial suppliers. All of the solvents for the photophysical measurements were of spectroscopic grade and obtained from Sigma-Aldrich. $[Co^{III}(dmgH)_2(py)(Cl)]^{\pm 0}$ [31] and $[Co^{III}(dmgH)_2(Cl)_2]^{1-}$ [32] were prepared and purified according to published procedures. The water for pulse radiolysis experiment was taken from a milli-Q plus ultrapure water system (Millipore).

Steady State Absorption and Emission Spectroscopy. Absorption spectra were measured with a Lambda 2 (Perkin-Elmer) UV−vis spectrometer. The spectra were recorded between 250 and 1000 at 480 nm per min with a 1.0 nm spectral bandwidth. The sample was contained in a 10 mm quartz cuvette. Fully corrected emission spectra were recorded on a FluoroMax-3 spectrometer (Horiba JobinYvon). To avoid aggregation and inner-filter effects, the absorption was adjusted to 0.05 at the excitation wavelength. Fluorescence quantum yields were determined by the comparative method[33] using *meso*-tetraphenylporphyrin (TPP) (Φ = 0.11 in toluene[34]) or zinc *meso*-tetraphenylporphyrin (ZnTPP) (Φ = 0.03 in toluene[34]) as standards.

Time Resolved Fluorescence Spectroscopy. Fluorescence lifetimes were determined by the time correlated single photon counting technique using a FlouroLog3 emission spectrometer (Horiba JobinYvon) equipped with an R3809U-58 MCP (Hamamatsu) and an N-405L laser diode (Horiba JobinYvon) exciting at 403 nm (≤200 ps fwhm).

Transient Absorption. In Erlangen, transient absorption (TA) experiments were carried out with an amplified Ti:Sapphire laser system CPA-2101 fs laser (Clark MXR: output 775 nm, 1 kHz, and 150 fs pulse width) using a transient absorption pump/probe detection system (TAPPS Helios, Ultrafast Systems). The 550 nm excitation wavelength was generated with a noncollinear optical parametric amplifier (NOPA, Clark MXR). The 256 nm excitation wavelength was formed by third harmonic generation. For both, excitation

dx.doi.org/10.1021/jp311766s | J. Phys. Chem. C 2013, 117, 1647−1655

wavelength pulse widths of <150 fs and energies of 100 nJ/pulse (550 nm) and 40 nJ/pulse (256 nm), respectively, were selected. TA experiments were also carried out in Rochester, NY, using an amplified Ti:sapphire laser (Spectra-Physics Spitfire, 800 nm, 2.25 mJ, 120 fs pulse) that pumped a home-built NOPA. The NOPA produced 100 nJ/pulse at 550 nm and provided time resolution of 300−400 fs when combined with an uncompressed continuum generated by focusing the 800 nm beam into a 2 mm thick CaF_2 window. Signals were detected with CCD (Princeton Instruments) after dispersion in a home-built prism spectrograph. The estimated error of the rate constants determined by transient absorption measurements is ±15%.

Pulse Radiolysis. The samples were saturated with N_2 and irradiated with high energy electron pulses (1 MeV, 15 ns duration) generated by a pulse transformer electron accelerator ELIT (Institute of Nuclear Physics, Novosibirsk, Russia). The dose delivered per pulse was measured with electron dosimetry, and pulses of 100 Gy per pulse were selected. The detection of the transient species was carried out using an optical absorption technique, consisting a pulsed (pulser MSP 05, Müller Elektronik-Optik) xenon lamp (XBO 450, Osram), a SpectraPro 500 monochromator (Acton Research Corporation), an R4220 photomultiplier (Hamamatsu Photonics), and a 500 MHz digitizing oscilloscope (TDS 640, Tektronix). A more detailed description of the setup used can be found elsewhere.[35]

Electrochemistry. Electrochemical data were obtained by square wave voltammetry using an EG&G Princeton Applied Research potentiostat in combination with a three electrode system. The counter electrode consisted of a platinum wire, and the working electrode was glassy carbon, while silver wire was used as a reference electrode. The measurements were carried out in anhydrous and argon saturated tetrahydrofuran. Tetrabutylammonium hexafluorophosphate was used as an auxiliary electrolyte (0.1 M). All potentials are referenced to ferrocene/ferrocenium as reference.

RESULTS AND DISCUSSION

Synthesis and Characterization. The synthesis of compounds **1**,[36] **2**,[37] and **3**[38] has been reported previously. Starting from **1**, **2**, and **3**, the corresponding cobaloximes **1Co**, **2Co**, and **3Co** were prepared in a straightforward manner by reacting $[Co^{III}(dmgH)_2(Cl)_2]^{1-}$ with the appropriate pyridyl substituted porphyrins or corrole in methanol at room temperature; see Scheme 1. A more detailed description of the synthesis and the analytical characterization is given in the Supporting Information.

The desired products were precipitated and isolated by filtration. Coordination of $[Co^{III}(dmgH)_2(Cl)_2]^{1-}$ to **1**, **2**, and **3** was confirmed by the changes observed in the aromatic region of the ^1H NMR spectra and by the appearance of a characteristic singlet resonance at 2.5 ppm attributed to the methyl groups of the dimethylglyoxime ligands (see Supporting Information). As seen in Figure S1.2 in the Supporting Information, which shows the aromatic region of the ^1H NMR spectra of **1** and **1Co**, coordination of cobaloxime to **1** results in considerable upfield shifts of the proton resonances.

Photophysical, Electrochemical, and Radiation Chemical Studies. The absorption spectra of pyridyl-substituted porphyrins **1** and **2** and the pyridyl-substituted corrole **3** are shown along with those of the corresponding $[Co^{III}(dmgH)_2(py)(Cl)]^{\pm0}$ hybrids, namely, **1Co**, **2Co**, and **3Co**, in Figures 1 (**2**/**2Co**), S2.1 in the Supporting Information (**1**/**1Co**), and S2.2 in the Supporting Information (**3**/**3Co**). In addition, a collection of the photophysical properties of the above compounds can be found in Table S4.1 in the Supporting Information. The spectrum of **2** shows Soret- and Q-band absorptions of a zinc porphyrin. In particular, the Soret-band absorption maximum was found in THF at 425 nm followed by Q-band absorptions that maximize at 556 and 596 nm. For **2Co**, a red-shifted Soret-band (i.e., 428 nm) and Q-bands (i.e., 558 and 600 nm) evolve in THF—Figure 1—which corroborates the coordination of cobaloxime. Porphyrin **1** reveals the expected spectrum for a free-base porphyrin featuring one Soret-band at 417 nm and four Q-bands at 513, 547, 590, and 646 nm in THF. As seen for **2Co**, the absorptions of **1Co** are red-shifted compared to **1** resulting in one Soret-band at 421 nm and four Q-bands at 515, 551, 591, and 648 nm in THF: Figure S2.1 in the Supporting Information.

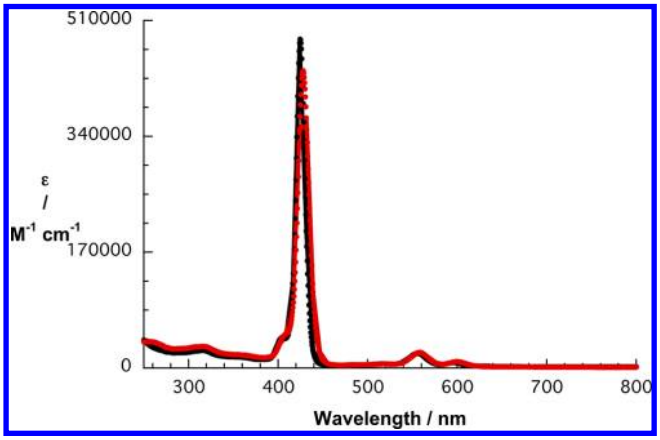

Figure 1. Absorption spectra of **2** (black line) and **2Co** (red line) in THF.

Corrole **3** possesses in THF one major maximum at 421 nm, which is further accompanied by two minor maxima at 567 and 609 nm as well as two shoulders at 519 and 640 nm: Figure S2.2 in the Supporting Information. In contrast to the subtle changes seen between **1Co** and **2Co**, on one hand, and **1** and **2**, on the other hand, the absorption spectrum of **3Co** differs strongly from that seen for **3**. For example, a maximum at 421 nm, a minor absorption at 633 nm, and a shoulder at 735 nm are observed for **3Co**, Figure S2.2 in the Supporting Information. Notably, the $[Co^{III}(dmgH)_2(py)(Cl)]^{\pm0}$ reference exhibits an absorption that starts around 500 nm and increases in intensity in the UV region: Figure 2, upper part.

In summary, **1** and **2** give rise upon coordination of $[Co^{III}(dmgH)_2(py)(Cl)]^{\pm0}$ to only minor red shifts of the absorptions. We consider this as evidence for minor electronic interactions between the building blocks in the ground state. Please note that analogous behavior has been observed for other porphyrin/cobaloxime conjugates.[23] In stark contrast, coordination of $[Co^{III}(dmgH)_2(py)(Cl)]^{\pm0}$ to **3** results in drastic changes of the absorption spectrum indicating appreciable interactions even in the ground state.

Next, the electrochemical properties of **1**, **2**, **3**, and $[Co^{III}(dmgH)_2(py)(Cl)]^{\pm0}$ were probed by means of square wave voltammetry in THF and were compared to those of **1Co**, **2Co**, and **3Co**. On the oxidative side, **1**, **2**, and **3** reveal two one electron oxidations at 0.68/0.78, 0.55/0.79, and 0.44/0.60 V,

dx.doi.org/10.1021/jp311766s | J. Phys. Chem. C 2013, 117, 1647−1655

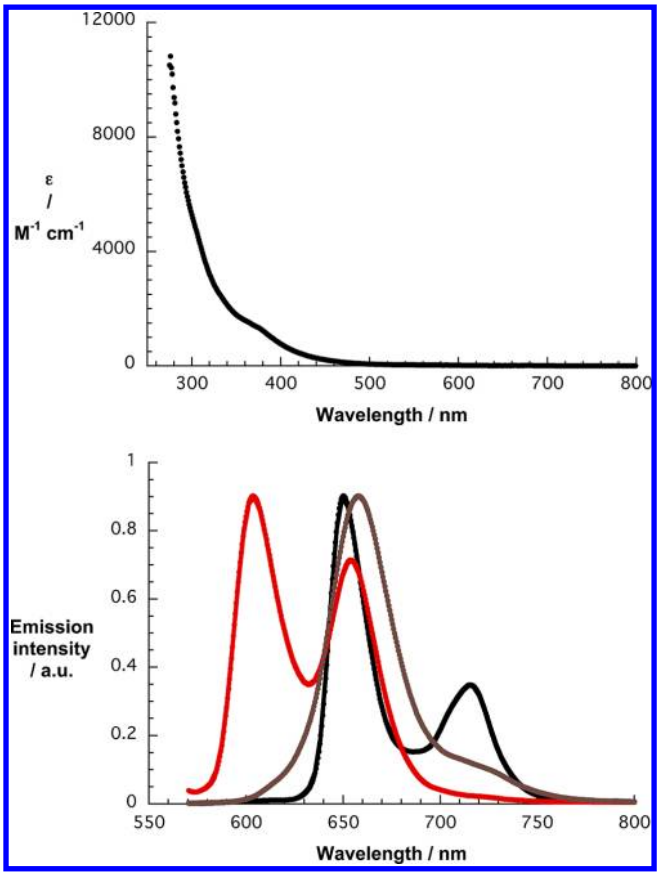

Figure 2. Upper part: Absorption spectrum of $[Co^{III}(dmgH)_2(py)(Cl)]^{\pm0}$ in acetonitrile. Lower part: Emission spectra of **1** (black line), **2** (red line), and **3** (brown line) in THF (normalized at the same maximum intensity).

respectively, to afford the corresponding radical cations and dications, while one electron reductions were seen at −1.53, −1.80, and −2.11 for **1**, **2**, and **3**, respectively. These values are in excellent agreement with those reported in the literature.[39] For $[Co^{III}(dmgH)_2(py)(Cl)]^{\pm0}$, reductions at −0.75, −1.14 (irreversible), and −1.66 (reversible) V were observed. In **1Co**, **2Co**, and **3Co**, the presence of $[Co^{III}(dmgH)_2(py)(Cl)]^{\pm0}$ evokes nearly no appreciable shifts in terms of the oxidations with values 0.63/0.73 V for **1Co**, 0.58/0.78 V for **2Co**, and 0.49/0.67 V for **3Co**. A shift toward more positive oxidation potentials emerged for **2Co** and **3Co**, while the oxidation in **1Co** appears easier. Nevertheless, the overall shifts are minor. Likewise, the $[Co^{III}(dmgH)_2(py)(Cl)]^{\pm0}$ centered reduction is not noticeably impacted in **1Co**, **2Co**, and **3Co** with its first reduction potential around −0.75. In conclusion, $[Co^{III}(dmgH)_2(py)(Cl)]^{\pm0}$, on one hand, and **1**, **2**, and **3**, on the other hand, do not feature in **1Co**, **2Co**, and **3Co** any mutual electronic communication. Table 1 summarizes the redox potentials for **1**, **2**, **3**, $[Co^{III}(dmgH)_2(py)(Cl)]^{\pm0}$, **1Co**, **2Co**, and **3Co**.

As a complement to the square wave voltammetric experiments, **1**, **2**, **3**, and $[Co^{III}(dmgH)_2(py)(Cl)]^{\pm0}$ were probed in spectroelectrochemical experiments. In particular, when applying potentials between 0.6 and 0.8 V the radical cations of **1**, **2**, and **3** were generated. For **1**, the differential absorption spectra of the radical cation feature maxima at 540, 575, 630, 670, and 690 nm, while minima evolve at 550, 600, and 650 nm. Similarly, the radical cation formation in the case

Table 1. Electrochemical Features of 1, 2, 3, $[Co^{III}(dmgH)_2(py)(Cl)]^{\pm0}$, 1Co, 2Co, and 3Co Determined by Means of Square Wave Voltammetry in THF[a]

compd	E_{OX2},[b] V	E_{OX1}, V	E_{RED1}, V	E_{RED2}, V	E_{RED3}, V
1	0.78	0.68	−1.53		
1Co	0.73	0.63			
2	0.79	0.55	−1.80		
2Co	0.78	0.58			
3	0.60	0.44	−2.11		
3Co	0.67	0.49			
$[Co^{III}(dmgH)_2(py)(Cl)]^{\pm0}$			−0.75	−1.14	−1.66

[a]All potentials are referred to Fc/Fc^+. [b]The estimated error for all potentials is ±0.01 V.

of **2** is accompanied by broad absorptions between 600 and 800 nm and bleaching at 560 nm.[40,41] In the case of **3**, characteristics of the radical cation include minima at 425, 570, and 623 nm—as a reflection of the ground state maxima—and maxima at 460 and approximately at 730 nm. These values are in good agreement with data for *meso*-substituted corroles.[42,43]

In terms of reducing $[Co^{III}(dmgH)_2(py)(Cl)]^{\pm0}$ at, for example, a potential of −0.8 V versus Fc/Fc^+, new major maxima arise at 315 and 425 nm accompanied by a broad maximum ranging from 470 to 570 nm. Notable, however, is the irreversibility of the reduction. To this end, applying a potential sufficient to reoxidize the reduced form of with $[Co^{III}(dmgH)_2(py)(Cl)]^{\pm0}$ failed to reinstate the ground state absorption. Instead, only the 426 nm feature decreased slightly in intensity, while the 315 nm feature further increased. At this point, we conclude that even in $[Co^{III}(dmgH)_2(py)(Cl)]^{\pm0}$ the one electron reduced form is subject to further chemical processes.

To verify the electrochemical reduction of $[Co^{III}(dmgH)_2(py)(Cl)]^{\pm0}$, pulse radiolysis experiments under reducing conditions were deemed necessary. All investigations were conducted in N_2-saturated, aqueous solutions containing 5 vol % 2-propanol. Such conditions led to the production of three highly reactive species, namely, $^{\bullet}H$, $^{\bullet}OH$, and e_{aq}^-, besides molecular products such as H_2 or H_2O_2. The function of 2-propanol is to efficiently scavenge $^{\bullet}OH$ and $^{\bullet}H$ radicals via hydrogen abstraction. The main resulting radical, that is, $(CH_3)_2{}^{\bullet}COH$, is a powerful reductant. The reaction of $[Co^{III}(dmgH)_2(py)(Cl)]^{\pm0}$ with e_{aq}^- was directly monitored via the decay of the e_{aq}^- transient absorption band maximizing around 720 nm, whose decay is giving rise to a new transient absorption with maxima at 470 and 630 nm: Figure 3. We ascribe this transient absorption to the one electron reduced form of $[Co^{III}(dmgH)_2(py)(Cl)]^{\pm0}$. Interestingly, no second formation kinetics for the one electron reduced $[Co^{III}(dmgH)_2(py)(Cl)]^{\pm0}$ is seen throughout our experiments. We must assume that either $(CH_3)_2{}^{\bullet}COH$ is incapable of reducing $[Co^{III}(dmgH)_2(py)(Cl)]^{\pm0}$ or the reaction is slower than the subsequent decay of the one electron reduced form of $[Co^{III}(dmgH)_2(py)(Cl)]^{\pm0}$. As the concentration of $[Co^{III}(dmgH)_2(py)(Cl)]^{\pm0}$ was increased from 1.25×10^{-4} to 5×10^{-4} M, the respective first-order rate constant for the decay of e_{aq}^- reveals a linear relationship with respect to the $[Co^{III}(dmgH)_2(py)(Cl)]^{\pm0}$ concentration. From the latter a bimolecular rate constant of 2.8×10^{10} M^{-1} s^{-1} was derived for the reduction of $[Co^{III}(dmgH)_2(py)(Cl)]^{\pm0}$ by e_{aq}^-. This rate

dx.doi.org/10.1021/jp311766s | J. Phys. Chem. C 2013, 117, 1647−1655

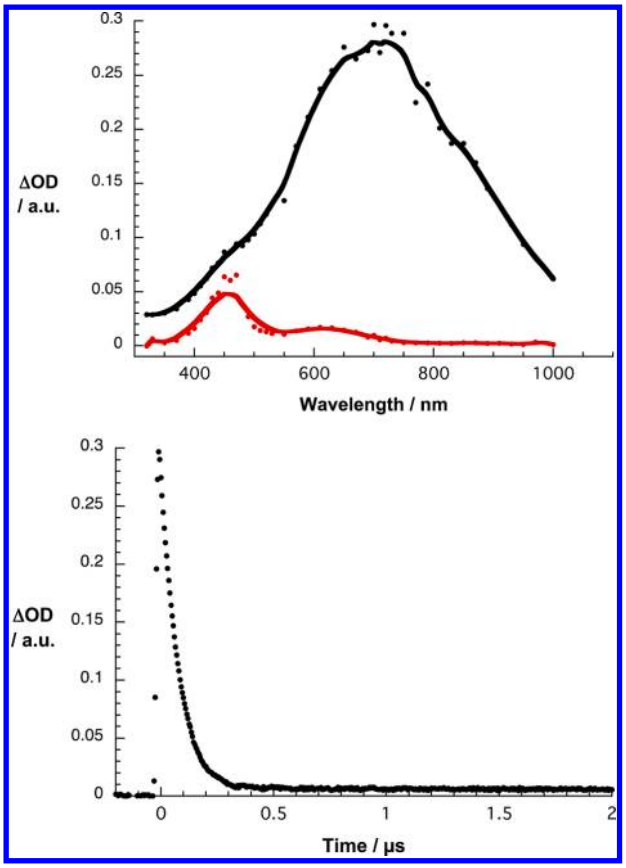

Figure 3. Upper part: Differential absorption spectra of $[Co^{III}(dmgH)_2(py)(Cl)]^{\pm 0}$ (5×10^{-4} M) in aqueous solution containing 2-propanol (10 vol %) saturated with N_2 upon pulse radiolysis (100 Gy/pulse) at different times (black spectrum, 75 ns, and red spectrum, 1 μs) after the electron pulse. Lower part: Corresponding time−absorption profile at 700 nm showing the decay of the solvated electron.

constant suggests a diffusion limited reaction without any substantial activation barrier.[44]

First insights into possible electron donor−acceptor interactions between the different constituents in the $[Co^{III}(dmgH)_2$(py-porphyrin)$(Cl)]^{\pm 0}$ and $[Co^{III}(dmgH)_2$(py-corrole)$(Cl)]^{\pm 0}$ hybrids came from fluorescence assays. In reference experiments, the fluorescence spectra of **1** and **2** showed the typical fluorescence features of free-base and zinc porphyrins, respectively. **2**, for example, exhibits two fluorescence maxima at 604 and 654 nm (2.1 eV), whereas maxima at 650 and 715 nm (1.9 eV) evolve for **1**. In Figure 4 and Figures S3.1 and S3.2 in the Supporting Information the fluorescence spectra of **2**/**2Co**, **1**/**1Co**, and **3**/**3Co** are compared, respectively. Importantly, the fluorescence patterns of just the porphyrins (i.e., **1** and **2**) and of their corresponding cobaloxime hybrids (i.e., **1Co** and **2Co**) are essentially identical with maxima that shift in THF to 653 and 717 nm for **1Co** and to 609 and 656 nm for **2Co**. On the contrary, the presence of cobaloxime induces in **1Co** and **2Co** a strong quenching of the porphyrin centered fluorescence: quantum yield of 0.054 versus 0.0026 (**1**/**1Co**) and 0.038 versus 0.0032 (**2**/**2Co**). For the corrole-based systems, the fluorescence underwent a red shift from 658 nm (1.9 eV) in **3** to 663 nm in **3Co** and the fluorescence quantum yields decrease from 0.078 in **3** to 0.0016 in **3Co** (Table S4.1 in the Supporting Information).

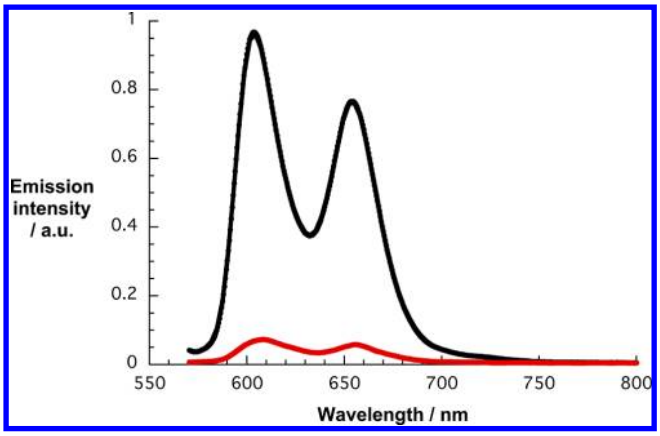

Figure 4. Fluorescence spectra of **2** (black spectrum) and **2Co** (red spectrum) in THF upon 550 nm photoexcitation.

In addition to the fluorescence spectra, fluorescence lifetimes were determined: Table S4.1 in the Supporting Information. For **1** and **1Co** fluorescence lifetimes of 10.4 and 0.4 ns were derived, respectively: Figure S4.1 in the Supporting Information. The fluorescence lifetimes for **2** and **2Co** were 1.9 and 0.1 ns respectively: Figure 5. Please note that the actual fit reveals

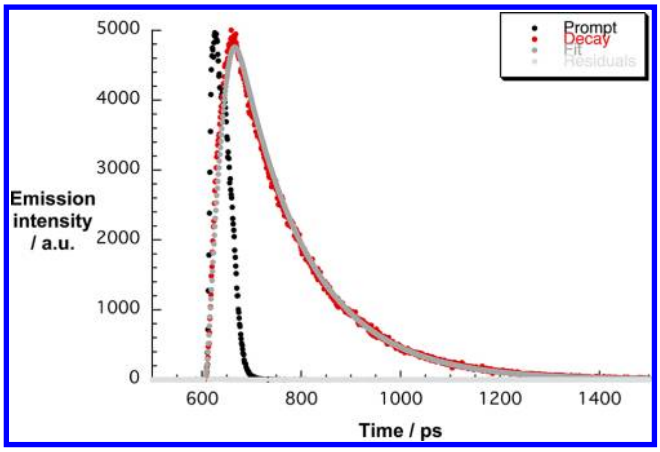

Figure 5. Fluorescence time profiles of **2Co** at 610 nm (red line) and the corresponding (biexponential) fit (gray line) including the IRF (black line) in THF upon 403 nm photoexcitation.

for **2Co** two lifetimes, that is, 1.9 and 0.1 ns. The earlier is, however, assumed to relate to residual traces of **2** that are present in **2Co**. The fluorescence lifetime of **3** was 3.1 ns. **3Co** rendered unstable and gave rise to decomposition during the TCSPC based fluorescence lifetime measurements. At this point of the investigation we reached the conclusion that the fluorescence quenching in **1Co**, **2Co**, and **3Co** must be due to an electron transfer and/or energy transfer deactivation. However, given the lack of spectral overlap between the absorption of $[Co^{III}(dmgH)_2(py)(Cl)]^{\pm 0}$, on one hand, and the fluorescence of **1**, **2**, and **3**, on the other hand, a Förster type energy transfer is unlikely to happen: Figure 2.

As a matter of fact, we determined the thermodynamic driving force for an intramolecular charge separation from the first singlet excited state of **1**, **2**, and **3** to $[Co^{III}(dmgH)_2(py)(Cl)]^{\pm 0}$ in **1Co**, **2Co**, and **3Co** by using the Rehm−Weller equation[45] 1.

$$\Delta G_{ET} = e_0(E_{OX} - E_{RED} - E_D + w) \quad (1)$$

dx.doi.org/10.1021/jp311766s | J. Phys. Chem. C 2013, 117, 1647−1655

Here, ΔG_{ET} is the free energy change for the charge separation, e_0 is the elementary electron charge, E_{OX} is the oxidation potential of the electron donor, E_{RED} is the reduction potential of the electron acceptor, E_D is the energy of the first singlet excited state of the donor group, and w represents the stabilization due to Coulomb attraction in the resulting ion pair, which varies from −0.15 eV for a closely associated ion pair in an exciplex to zero if the components are spatially well separated. E_{OX} and E_{RED} were taken from the electrochemical experiments. Using the data given in Table 1 and taking −0.06 eV as a reasonable estimate for the Coulomb attractions in polar solvents, since the components are neither closely associated or well separated,[46] we obtain ΔG_{ET} values of −0.47 ± 0.02, −0.83 ± 0.02, and −0.75 ± 0.02 eV for charge separation from the first singlet excited state of **1**, **2**, and **3** to cobaloxime, that is, reduction of Co^{III} to Co^{II}, for **1Co**, **2Co**, and **3Co**, respectively. In other words, charge separation seems slightly favorable in **1Co** and clearly favorable in **2Co** and **3Co**. Therefore, we reach the tentative conclusion that the fluorescence quenching observed in **1Co**, **2Co**, and **3Co** must relate to an intramolecular charge separation.

Deeper insights into the nature of the mechanism of the fluorescence quenching came from transient absorption spectroscopy. Toward this end, **1**, **2**, and **3** were excited with fs-laser pulses at 550 nm and compared to **1Co**, **2Co**, and **3Co**. **1** and **2** showed a strong transient bleaching after the laser pulse in the regions around 420 and 520 nm suggesting consumption of the porphyrin singlet ground states as a result of forming the corresponding singlet excited states. An immediately formed absorption accompanies the bleaching. For example, the singlet excited state of **2** exhibits new absorption bands between 420 and 900 nm with maxima at 460, 580, 620, 700, and 825 nm and minima at 555 and 600 nm, which mirrors the ground state absorption: Figure 6. This transient absorption correlates with the singlet excited state of **2**. The transient absorption of the singlet excited state of **1** shows absorption bands between 420 and 900 nm with maxima at 435, 535, 575, 620, 695, 760, and 825 nm and minima at 515, 550, 600, and 650 nm: Figure S5.1 in the Supporting Information. Importantly, the latter mirrors the ground state absorption. The singlet transients produced upon photoexcitation decay with lifetimes of around 9.8 and 2.1 ns for **1** and **2**, respectively, via intersystem crossing into the corresponding triplet manifolds. The main spectral features of the latter state include maxima at 440/770 nm (**1**) and 460/840 (**2**). For **3**, the singlet excited and triplet excited state features, Figure S5.2 in the Supporting Information, include maxima at 465/820 and 463 nm, respectively, while the minimum remains at 550 nm. The singlet lifetime for **3** is 2.7 ns. The singlet exited state lifetimes measured for **1**, **2**, and **3** agree well with those determined by time correlated fluorescence measurements.

Photoexcitation of $[Co^{III}(dmgH)_2(py)(Cl)]^{\pm 0}$ with fs-laser pulses at 256 nm leads to the instantaneous formation of a transient absorption that features a maximum in the visible region around 490 nm. This transient absorption decays rather fast with a lifetime of 5 ps back to the ground state: Figure 7.

When turning to the corresponding $[Co^{III}(dmgH)_2(py\text{-}porphyrin)(Cl)]^{\pm 0}$ and $[Co^{III}(dmgH)_2(py\text{-}corrole)(Cl)]^{\pm 0}$ hybrids, the same singlet excited state features evolve that were already seen in the experiments with the porphyrin references (i.e., **1** and **2**) and the corrole reference (i.e., **3**) despite the presence of cobaloxime. In particular, ground state bleaching of the Soret- and Q-bands is seen in the 400 to 450 and 500 to 600 nm regions, respectively, accompanied by new transients that were detected throughout the entire visible range: Figure 8 and Figures S5.3 and S5.4 in the Supporting Information. These singlet excited state features decay with monoexponential and solvent dependent dynamics. For example, from multiple wavelength analyses of **2Co** we derived lifetimes of 81 ± 2 and 63 ± 3 ps in toluene and THF, respectively. For **1Co**, the corresponding lifetimes are 380 ± 5 ps (toluene) and 410 ± 5 ps (THF), while the lifetimes are 680 ± 5 ps (toluene) and 470 ± 5 ps (THF) for **3Co**. Interestingly, the monoexponential decay leads to the regeneration of the singlet ground state without the formation of any appreciable photoproduct. This excited state behavior is in sharp contrast to the slow singlet excited state decay via intersystem crossing observed for **1** (9.8 ns), **2** (2.1 ns), and **3** (2.7 ns) leading to the formation of the corresponding triplet excited state as shown by the characteristic fingerprints for **1** (i.e., 440/770 nm) and **2** (i.e., 460/840 nm). A reasonable interpretation of the aforementioned is a charge separation process to yield the oxidized porphyrins/corrole and the reduced $[Co^{III}(dmgH)_2(py)(Cl)]^{\pm 0}$ in **1Co**, **2Co**, and **3Co**. While this process is well-known for porphyrin systems, the possibility of charge separation in various dyads and triads based on corroles was only recently described.[47,48] A much faster charge recombination process follows the latter. Further support for this interpretation is provided by the much faster decay of the porphyrin-based first singlet excited state in

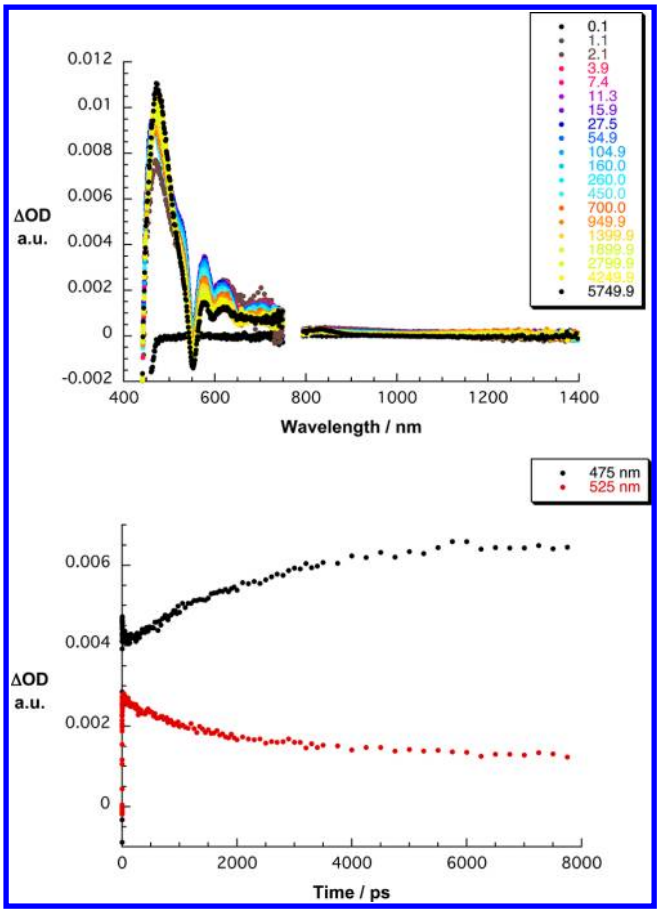

Figure 6. Upper part: Differential absorption spectra (visible and NIR) obtained upon femtosecond flash photolysis (550 nm, 100 nJ/pulse) of **2** in THF with several time delays between 0.1 and 5749.9 ps at room temperature. Lower part: Time−absorption profiles of the spectra shown above at 475 nm (black line) and 525 nm (red line).

dx.doi.org/10.1021/jp311766s | J. Phys. Chem. C 2013, 117, 1647−1655

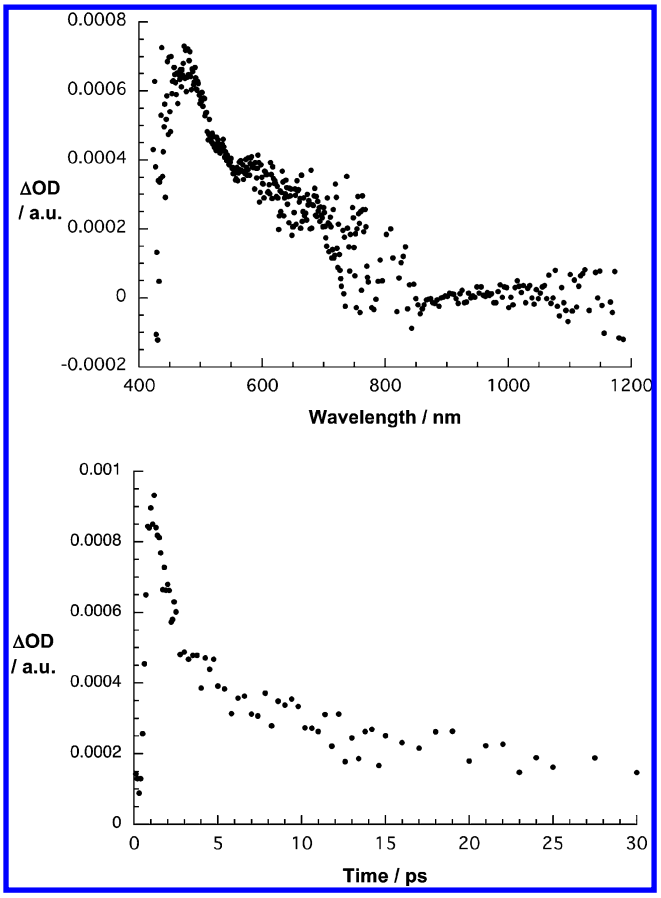

Figure 7. Upper part: Differential absorption spectra (visible and NIR) obtained upon femtosecond flash photolysis (256 nm, 40 nJ/pulse) of $[Co^{III}(dmgH)_2(py)(Cl)]^{\pm 0}$ in acetonitrile with a time delay of 2 ps. Lower part: Time−absorption profile of the spectra shown above at 490 nm.

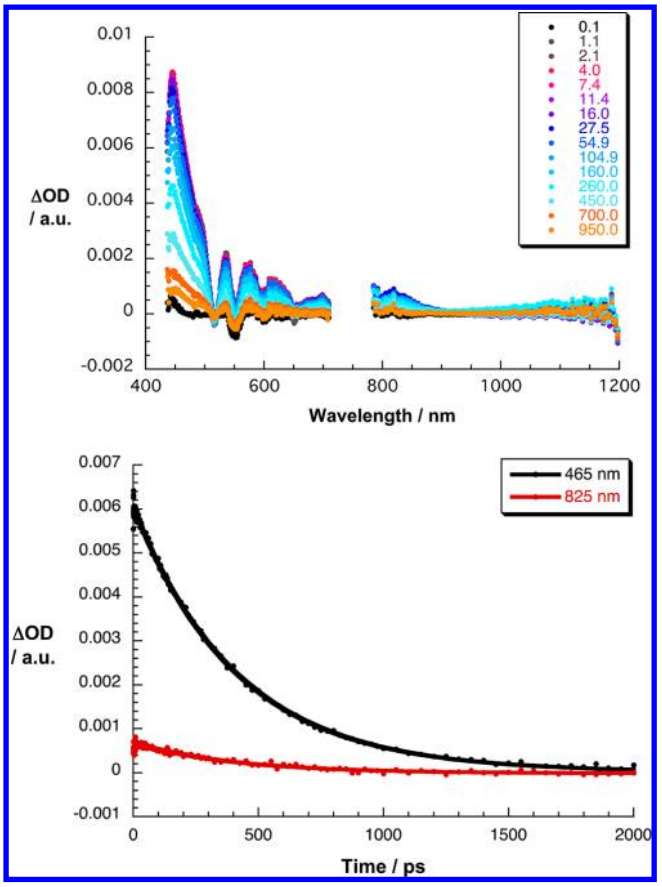

Figure 8. Upper part: Differential absorption spectra (visible and NIR) obtained upon femtosecond flash photolysis (550 nm, 100 nJ/pulse) of **2Co** in THF with several time delays at room temperature. Lower part: Time−absorption profiles of the spectra shown above at 465 nm (black line) and 825 nm (red line).

2Co compared to **1Co**, which correlates with the more favorable driving force for charge separation predicted for the former, vide supra.

To further corroborate our charge separation/charge recombination hypothesis, triethylamine (TEA) was added as a sacrificial electron donor in excess of 1000 times. The addition exerted no appreciable influence on the initial formation of the porphyrin singlet excited states, but led to a slight acceleration on their monoexponential decay dynamics. As an example, the lifetimes of **2Co** in toluene are 81 ± 2 and 66 ± 4 ps in the absence and presence of TEA, respectively. In **1Co**, the corresponding lifetimes are 380 ± 5 ps and 350 ± 15 ps.

Hydrogen Evolution Studies. Experiments to assess the photocatalytic activity of **1Co**, **2Co**, and **3Co** toward hydrogen production were performed in deoxygenated THF/H_2O (4:1) solutions with triethylamine (TEA) as sacrificial donor. These conditions essentially reproduce the conditions selected in a recent study by Sun and co-workers.[23] In agreement with the reported results,[23] between the two porphyrins, namely, **1Co** and **2Co**, only the system featuring ZnP as electron donor reveals photocatalytic activity. **1Co** and the corrole containing system **3Co** lack any appreciable hydrogen evolution. **2Co** provides in the presence of 1000 equiv of TEA the largest amount of H_2 after 24 h of irradiation. It is worth noting that the amount of hydrogen produced by our binuclear complex is far less than that reported for the system of Sun and co-workers.[23] According to the proposed mechanism for hydrogen production by cobaloxime catalysts,[20,21,25,29,30] it is postulated in the literature that the key step involves the generation of a catalytically active Co^I species. As shown in Scheme 2 this may occur via an oxidative or reductive pathway. Both pathways produce the radical cation of TEA, which decomposes through proton loss, electron transfer, and hydrolysis to diethylamine and acetaldehyde.[49] Our photophysical results show that the reduction of Co^{III} to Co^{II} takes place through rapid electron transfer from the singlet state of the **1**, **2**, or **3** to **1Co**, **2Co**, and **3Co**, respectively. However, in the absence of a sacrificial donor, a rapid charge recombination leads back to the initial species. A thermodynamic analysis using the Rehm−Weller equation shows that further reduction of Co^{II} to Co^I is endergonic in both compounds **1Co** and **2Co** with values of 0.53 ± 0.02 and 0.09 ± 0.02 eV, respectively. On this basis, the observed hydrogen production in systems such as **2Co** is usually explained in the literature by the generation of the Co^I species.[17,26,50] The typical explanation according to the literature[42] for the formation of the latter is by a reductive pathway possibly facilitated by coordination of TEA to **2Co**[23] as described in Scheme 2, vide infra.

CONCLUSION

In this paper we reported the successful synthesis and photophysical characterization of porphyrin/$[Co^{III}(dmgH)_2(Cl)]^{\pm 0}$ and corrole/$[Co^{III}(dmgH)_2(Cl)]^{\pm 0}$ con-

dx.doi.org/10.1021/jp311766s | J. Phys. Chem. C 2013, 117, 1647−1655

Scheme 2. Proposed Photochemical Steps to the Production of Co^{I}[a]

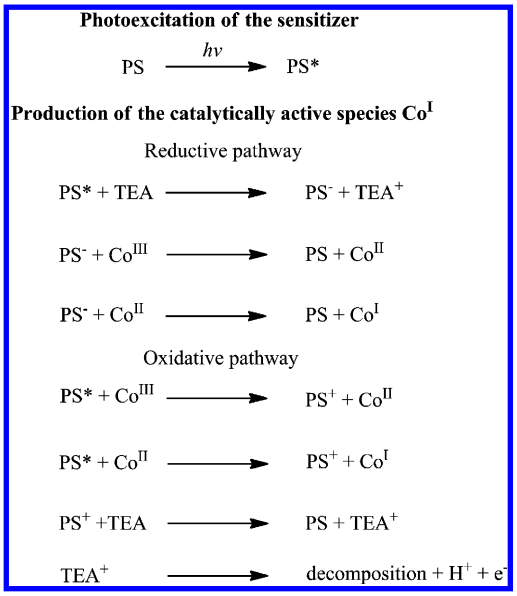

[a]TEA stands for triethylamine and PS for photosensitizer in particular chromophore **2** in **2Co**.

jugates as potential hydrogen forming entities in aqueous media. The main finding is that with this molecular design in the hybrid systems selective excitation of the porphyrin or corrole chromophore is followed by the formation of a charge separated state whose lifetime is much shorter than the lifetime of the quenched singlet excited state of the sensitizing porphyrins/corrole. As a direct consequence of the latter no significant concentration of the charge-separated state builds up during steady state illumination. In addition, the fairly short-lived charge-separated state appears to be counterproductive in terms of inducing the water splitting.

We take the aforementioned as a basis to rationalize the long induction period noted in the hydrogen formation experiments, which reach up to 24 h of illumination. In fact, we hypothesize that the hydrogen formation might not be due to electron transfer from the porphyrins/corrole to $[Co^{III}(dmgH)_2(py)(Cl)]^{\pm 0}$ but rather due to direct excitation of $[Co^{III}(dmgH)_2(py)(Cl)]^{\pm 0}$. Such a mechanism implies the decomposition of the chromophore that happens predominantly during the induction period. It should be emphasized that a 400 nm long-path cutoff filter as used by Sun and coworkers[23] will not avoid or exclude direct excitation of $[Co^{III}(dmgH)_2(py)(Cl)]^{\pm 0}$ owing to the onset of the absorption around 500 nm as illustrated in Figure 2, upper part.

We proved that the axial coordination of the porphyrins/corrole features only limited efficiency and led to rather unstable photocatalysts under illumination. Bearing this in mind, different molecular designs may offer a solution (for example, association via covalent attachment to the oxime ligand rather than via axial coordination). Moreover, the one electron reduction of $[Co^{III}(dmgH)_2(py)(Cl)]^{\pm 0}$ seems to lead to an unstable intermediate, which shows a fairly complex reaction mechanism. Notably, the reduction of cobalt oxime complexes plays a major role in water splitting,[50] and, as such, a better understanding of these reactions is necessary. The latter will require a complex kinetic and spectroscopic study of the reduction of $[Co^{III}(dmgH)_2(py)(Cl)]^{\pm 0}$ and the reactivity of its reduced form. It is foreseeable that new insights will evolve as valuable guidelines toward a comprehensive understanding of the water splitting mechanism in $[Co^{III}(dmgH)_2]^{1+}$ type systems including reactive intermediates and rate constants. We strongly believe that a complete mechanistic understanding will pave the way to efficient and stable designs toward photocatalytic water splitting.

■ ASSOCIATED CONTENT

Supporting Information

Synthetic details, NMR spectra, UV−vis absorption and emission spectra, and additional transient absorption spectra. S1: The synthetic strategy, with NMR and elementary analysis data. S2: UV/vis absorption spectra of the free-base porphyrin (**1**) and the free-base porphyrin−cobaloxime hybrid (**1Co**) as well as the corrole reference compound (**3**) and the corrole−cobaloxime hybrid (**3Co**). S3: Fluorescence spectra of the free-base porphyrin (**1**) and the free-base porphyrin−cobaloxime hybrid (**1Co**) as well as the corrole reference compound (**3**) and the corrole−cobaloxime hybrid (**3Co**). S4: Fluorescence time profiles of the free-base porphyrin−cobaloxime hybrid (**1Co**) and steady state absorption and emission data as well as time-resolved emission data of **1**, **2**, **3**, **1Co**, **2Co**, and **3Co**. S5: Fs-transient absorption spectra and time profiles of the free-base porphyrin (**1**) and the free-base porphyrin−cobaloxime hybrid (**1Co**) as well as the corrole reference compound (**3**) and the corrole−cobaloxime hybrid (**3Co**). This material is available free of charge via the Internet at http://pubs.acs.org.

■ AUTHOR INFORMATION

Corresponding Author

*D.T.G.: Institute of Organic Chemistry, Polish Academy of Sciences, Kasprzaka 44/52, 01-224 Warsaw, Poland; e-mail, dtgryko@icho.edu.pl. A.G.C.: Chemistry Department, University of Crete, Voutes Campus, PO Box 2208, 71003 Heraklion, Crete, Greece; e-mail, coutsole@chemistry.uoc.gr. D.M.G.: Department of Chemistry and Pharmacy, Interdisciplinary Center for Molecular Materials (ICMM), Friedrich-Alexander-Universitaet Erlangen-Nuernberg, Egerlandstr. 3, 91058 Erlangen, Germany; e-mail, dirk.guldi@chemie.uni-erlangen.de.

Present Address

[§]Chemistry Department, University of Ioannina, Ioannina 45110, Greece.

Author Contributions

[¶]K.P. and T.L. contributed equally to the manuscript.

Notes

The authors declare no competing financial interest.

■ ACKNOWLEDGMENTS

The European Commission funded this research by FP7-REGPOT-2008-1, Project BIOSOLENUTI No. 229927, Heraklitos grant from Ministry of Education, and GSRT. In addition, financial support from the DFG (Cluster of Excellence and SFB 583), the Bavarian initiative "Solar Technologies go Hybrid", Polish Ministry of Science and Higher Education (Contract N204 123837) and the BMBF are greatly acknowledged. We would like to thank Prof. Abel and his group from the Leipzig University, Leipzig, Germany, for the support during the pulse radiolysis measurements.

■ ABBREVIATIONS

dmgH: dimethylglyoxime

$[Ru(bipy)_3]^{2+}$: ruthenium tris bipyridine
TPP: tetraphenylporphyrin
ZnTPP: zinc tetraphenylporphyrin
TEA: triethylamine

REFERENCES

(1) Nocera, D. G.; Teets, T. S. *Chem. Commun.* **2011**, *47*, 9268−9274.
(2) Nocera, D. G.; Cook, T. R.; Dogutan, D. K.; Reece, S. Y.; Surendranath, Y.; Teets, T. S. *Chem. Rev.* **2010**, *110*, 6474−6502.
(3) Lewis, N. S.; Nocera, D. G. *Proc. Natl. Acad. Sci. U.S.A.* **2006**, *103*, 15729−15735.
(4) Eisenberg, R. *Science* **2009**, *324*, 44−45.
(5) Gray, H. B. *Nat. Chem.* **2009**, *1*, 7−7.
(6) Sabatini, R. P.; McCormick, T. M.; Lazarides, T.; Wilson, K. C.; Eisenberg, R.; McCamant, D. W. *J. Phys. Chem. Lett.* **2011**, *2*, 223−227.
(7) Du, P. W.; Schneider, J.; Jarosz, P.; Zhang, J.; Brennessel, W. W.; Eisenberg, R. *J. Phys. Chem. B* **2007**, *111*, 6887−6894.
(8) Du, P.; Schneider, J.; Fan, L.; Zhao, W.; Patel, U.; Castellano, F. N.; Eisenberg, R. *J. Am. Chem. Soc.* **2008**, *130*, 5056−5058.
(9) Tinker, L. L.; McDaniel, N. D.; Curtin, P. N.; Smith, C. K.; Ireland, M. J.; Bernhard, S. *Chem.—Eur. J.* **2007**, *13*, 8726−8732.
(10) Merki, D.; Hu, X. L. *Energy Environ. Sci.* **2011**, *4*, 3878−3888.
(11) Hatay, I.; Ge, P. Y.; Vrubel, H.; Hu, X. L.; Girault, H. H. *Energy Environ. Sci.* **2011**, *4*, 4246−4251.
(12) Merki, D.; Fierro, S.; Vrubel, H.; Hu, X. L. *Chem. Sci.* **2011**, *2*, 1262−1267.
(13) Sun, L. C.; Akermark, B.; Ott, S. *Coord. Chem. Rev.* **2005**, *249*, 1653−1663.
(14) Wang, F.; Wang, W. G.; Wang, X. J.; Wang, H. Y.; Tung, C. H.; Wu, L. Z. *Angew. Chem., Int. Ed.* **2011**, *50*, 3193−3197.
(15) Wang, H. Y.; Wang, W. G.; Si, G.; Wang, F.; Tung, C. H.; Wu, L. Z. *Langmuir* **2010**, *26*, 9766−9771.
(16) Winkler, M.; Kawelke, S.; Happe, T. *Bioresour. Technol.* **2011**, *102*, 8493−8500.
(17) Du, P. W.; Eisenberg, R. *Energy Environ. Sci.* **2012**, *5*, 6012−6021.
(18) Artero, V.; Chavarot-Kerlidou, M.; Fontecave, M. *Angew. Chem., Int. Ed.* **2011**, *50*, 7238−7266.
(19) Lakadamyali, F.; Kato, M.; Muresan, N. M.; Reisner, E. *Angew. Chem., Int. Ed.* **2012**, *51*, 9381−9384.
(20) Dempsey, J. L.; Winkler, J. R.; Gray, H. B. *J. Am. Chem. Soc.* **2010**, *132*, 16774−16776.
(21) Winkler, J. R.; Dempsey, J. L.; Gray, H. B. *J. Am. Chem. Soc.* **2010**, *132*, 1060−1065.
(22) Brunschwig, B. S.; Dempsey, J. L.; Winkler, J. R.; Gray, H. B. *Acc. Chem. Res.* **2009**, *42*, 1995−2004.
(23) Wang, M.; Zhang, P.; Li, C. X.; Li, X. Q.; Dong, J. F.; Sun, L. C. *Chem. Commun.* **2010**, *46*, 8806−8808.
(24) McCormick, T. M.; Han, Z.; Weinberg, D. J.; Brennessel, W. W.; Holland, P. L.; Eisenberg, R. *Inorg. Chem.* **2011**, *50*, 10660−10666.
(25) McCormick, T. M.; Calitree, B. D.; Orchard, A.; Kraut, N. D.; Bright, F. V.; Detty, M. R.; Eisenberg, R. *J. Am. Chem. Soc.* **2010**, *132*, 15480−15483.
(26) Lazarides, T.; McCormick, T.; Du, P. W.; Luo, G. G.; Lindley, B.; Eisenberg, R. *J. Am. Chem. Soc.* **2009**, *131*, 9192−9194.
(27) Zhao, J. H.; Gong, L. M.; Wang, J.; Li, H.; Wang, L.; Zhu, Z. P. *Catal. Commun.* **2011**, *12*, 1099−1103.
(28) Wang, M.; Li, C.; Pan, J. X.; Zhang, P.; Zhang, R.; Sun, L. C. *J. Organomet. Chem.* **2009**, *694*, 2814−2819.
(29) Du, P. W.; Schneider, J.; Luo, G. G.; Brennessel, W. W.; Eisenberg, R. *Inorg. Chem.* **2009**, *48*, 4952−4962.
(30) Du, P. W.; Knowles, K.; Eisenberg, R. *J. Am. Chem. Soc.* **2008**, *130*, 12576−12577.
(31) Schrauzer, G. N. *Inorg. Synth.* **1968**, *11*, 61−70.
(32) Trogler, W. C.; Stewart, R. C.; Epps, L. A.; Marzilli, L. G. *Inorg. Chem.* **1974**, *13*, 1564−1570.
(33) Demas, J. N.; Crosby, G. A. *J. Phys. Chem.* **1971**, *75*, 991−1024.
(34) Seybold, P. G.; Gouterman, M. *J. Mol. Spectrosc.* **1969**, *31*, 1−13.
(35) Brede, O.; Orthner, H.; Zubarev, V.; Hermann, R. *J. Phys. Chem.* **1996**, *100*, 7097−7105.
(36) Gianferrara, T.; Giust, D.; Bratsos, I.; Alessio, E. *Tetrahedron* **2007**, *63*, 5006−5013.
(37) Chertkov, V. A.; Sirish, M.; Schneider, H. J. *Chem.—Eur. J.* **2002**, *8*, 1181−1188.
(38) Gryko, D. T.; Koszarna, B. *Synthesis* **2004**, 2205−2209.
(39) Kadish, K. M.; Smith, K. M.; Guilard, R. *The Porphyrin Handbook*; Academic: San Diego, CA, 2000.
(40) Krokos, E.; Spänig, F.; Ruppert, M.; Hirsch, A.; Guldi, D. M. *Chem.—Eur. J.* **2012**, *18*, 10427−10435.
(41) Krokos, E.; Schubert, C.; Spänig, F.; Ruppert, M.; Hirsch, A.; Guldi, D. M. *Chem. Asian J.* **2012**, *7*, 1451−1459.
(42) Ventura, B.; Degli Esposti, A.; Koszarna, B.; Gryko, D. T.; Flamigni, L. *New J. Chem.* **2005**, *29*, 1559−1566.
(43) Shen, J.; Shao, J.; Ou, Z.; E, W.; Koszarna, B.; Gryko, D. T.; Kadish, K. M. *Inorg. Chem.* **2006**, *45*, 2251−2265.
(44) Once the $[Co(dmgH)_2(py)(Cl)]$ is reduced, it is unstable and decays in a complex mechanism.
(45) Rehm, D.; Weller, A. *Isr. J. Chem.* **1970**, *8*, 259−271.
(46) Lakowicz, J. R. *Principles of Fluorescence Spectroscopy*, 3rd ed.; Springer Science+Business Media: New York, 2006.
(47) Flamigni, L.; Gryko, D. T. *Chem. Soc. Rev.* **2009**, *38*, 1635−1646.
(48) Tasior, M.; Gryko, D. T.; Pielacińska, D.; Zanelli, A.; Flamigni, L. *Chem. Asian J.* **2010**, *5*, 130−140.
(49) Kalyanasundaram, K.; Kiwi, J.; Gratzel, M. *Helv. Chim. Acta* **1978**, *61*, 2720−2730.
(50) Fihri, A.; Artero, V.; Razavet, M.; Baffert, C.; Leibl, W.; Fontecave, M. *Angew. Chem., Int. Ed.* **2008**, *47*, 564−567.